A Final Report

to the

NATIONAL AERONAUTICS AND SPACE ADMINISTRATION

on

A Study of Extended Zodiacal Structures

NASA Project Number NAG 5-1236

Period: 15 August 1989 through 14 August 1990

Contractor: Steward Observatory
University of Arizona

Investigator: Mark V. Sykes
Steward Observatory
University of Arizona
Tucson, AZ 85721
(602-621-2054)

Attention: Dr. Don West
Goddard Technical Officer
Goddard Space Flight Center
Greenbelt MD 20771

ABSTRACT

Observations of cometary dust trails and zodiacal dust bands, discovered by the Infrared Astronomical Satellite, have been analysed in a continuing effort to understand their nature and relationship to comets, asteroids, and processes effecting those bodies.

A survey of all trails observed by IRAS has been completed, and analysis of this phenomenon continues. A total of 8 trails have been associated with known short-period comets (Churyumov-Gerasimenko, Encke, Gunn, Kopff, Pons-Winnecke, Schwassmann-Wachmann 1, Tempel 1, and Tempel 2), and a few faint trails have been detected which are not associated with any known comet. It is inferred that all short-period comets may have trails, and that the trails detected were seen as a consequence of observational selection effects. Were IRAS launched today, it would likely observe a largely different set of trails. The Tempel 2 trail exhibits a small but significant excess in color temperature relative to a blackbody at the same heliocentric distance. This excess may be due to the presence of a population of small, low-β particles deriving from large particles within the trail, or a temperature gradient over the surface of large trail particles. Trails represent the very first stage in the formation and evolution of a meteor stream, and may also be the primary mechanism by which comets contribute to the interplanetary dust complex.

A mathematical model of the spatial distribution of orbitally evolved collisional debris was developed which reproduces the zodiacal dust band phenomena and was used in the analysis of dust band observations made by IRAS. This has resulted in the principal zodiacal dust bands being firmly related to the principal Hirayama asteroid families. In addition, evidence for the collisional diffusion of the orbital elements of the dust particles has been found in the case of dust generated in the Eos asteroid family. It is also found that the catastrophic disruption of the Koronis parent body was much more recent than that of the Eos and Themis parent bodies. Overall, analysis of this phenomenon has supported the thesis that dust production in the asteroid belt is a non-equilibrium process.

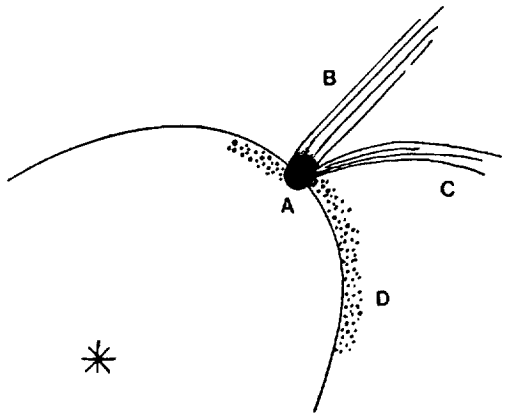

Figure 1. Comets generally exhibit a variety of phenomena at visual wavelengths including (a) the coma, (b) an ion tail, and (c) a dust tail. At thermal wavelengths a new phenomenon becomes apparent:(d) the dust trail, consisting of large particles moving slowly away from the nucleus along orbital paths very close to that of the parent comet.

Introduction

The Infrared Astronomical Satellite (IRAS) conducted the first sensitive survey of the sky at thermal infrared wavelengths. Over the course of this survey structures were observed in the zodiacal thermal emission which never before had been detected. These included the cometary dust trails (1) and zodiacal dust bands (2).

When we think of dust from comets, we think primarily of the tails sweeping away from the Sun, along with ion tails, forming the flowing "hair" from which comets derive their name. These particles tend to be micron-sized and are very sensitive to radiation pressure. Dust *trails*, on the other hand, consist of large particles, are relatively insensitive to radiation pressure, and cover portion of the orbits of short-period comets (Fig. 1). Trails were first detected by the Infrared Astronomical Satellite (1), and derive their name from their long, narrow appearance - sometimes extending tens of degrees across the sky while having a width of only a few arcminutes.

In 1983 the Tempel 2 dust trail was by far the most prominent such structure, as it came within 0.4 AU of the Earth while passing through perihelion. It was first detected as a string of 25 μm sources seeming related to periodic comet Tempel 2 (3). Subsequent analysis of these detections indicated that they may be low-velocity emissions of submillimeter particles (4). Sykes *et al.* (1) found that these point sources were actually part of a continuous stream of material extending behind as well as ahead of the comet. They also found trails associated with other short-period comets. Subsequent analysis determined that all trails consisted of large, refractory particles with small (m/sec) velocities relative to their parents (5).

The Tempel 2 trail has been the focus of a recent study (6) showing it to consist primarily of millimeter-sized particles, emitted at velocities of a few meters/sec over the past few hundred years. It also exhibits a small, but significant, enhancement in color temperature relative to that expected for a blackbody at the heliocentric distances observed. This is explained as either evidence for a population of small particles released from large particles, or for a temperature gradient across the large particle surfaces such that they are warmer towards the Sun. Number denisities are such that the Tempel 2 trail could pose a hazard to CRAF-type spacecraft moving within it (7).

The zodiacal dust bands were initially noticed as symmetrically placed "shoulders" on scans of the broad zodiacal thermal emission measured by IRAS at 12 and 25 μm (2). These bumps were found to form bands, roughly parallel to the ecliptic over all longitudes. Zodiacal dust bands consist of collisional debris located in the asteroid belt, and represents regions of contemporary dust production never before observed. The most prominent of these bands have been associated with the major Hirayama asteroid families (8). Early work indicated that it was probable that these and other fainter bands might arise from single catastrophic disruptions of moderate to small asteroids (9). Another hypothesis proposes that the bands arise from the global comminution of the entire asteroid belt, in which they represent the local enhancement of the volume density of asteroids, and do not represent a stochastic event. This has been reviewed in (10).

Cometary Dust Trails

The Survey

A systematic examination of the IRAS Skyflux Maps was undertaken in order to find all obvious dust trails observed by IRAS. This work began under a previous NASA grant, and continues under a new grant from the NASA Astrophysics Data Program. It was determined that in the 100 μm band trails were too faint and the infrared cirrus too bright to conduct the survey, so plates examined were restricted to images in the 12, 25, and 60 μm bands. Even then, the number of images to be visually inspected exceeds 1800, hence the extended effort of the project. Each image was inspected more than once, at different times, in order to increase reliability. Images containing trails were inspected additional times to double check positional information. As a consequence of stripe noise and confusion with other astrophysical sources (dust bands, cirrus), it was decided that an automated process for trail identification was not possible within the resources available to the investigation.

Equipment was provided by other sources which reproduced the image processing environment at the Infrared Processing and Analysis Center (IPAC). This afforded ease of access to the data and allowed us to utilize software developed by IPAC to analyse the IRAS images. Software was developed under this contract to project arbitrary elliptical orbits onto the IRAS data scan by scan and to plot these points onto IRAS images to compare the orbits of potential parent bodies to trails detected on the IRAS images. These projections took into account all parallactic effects, and superceded earlier software which projected

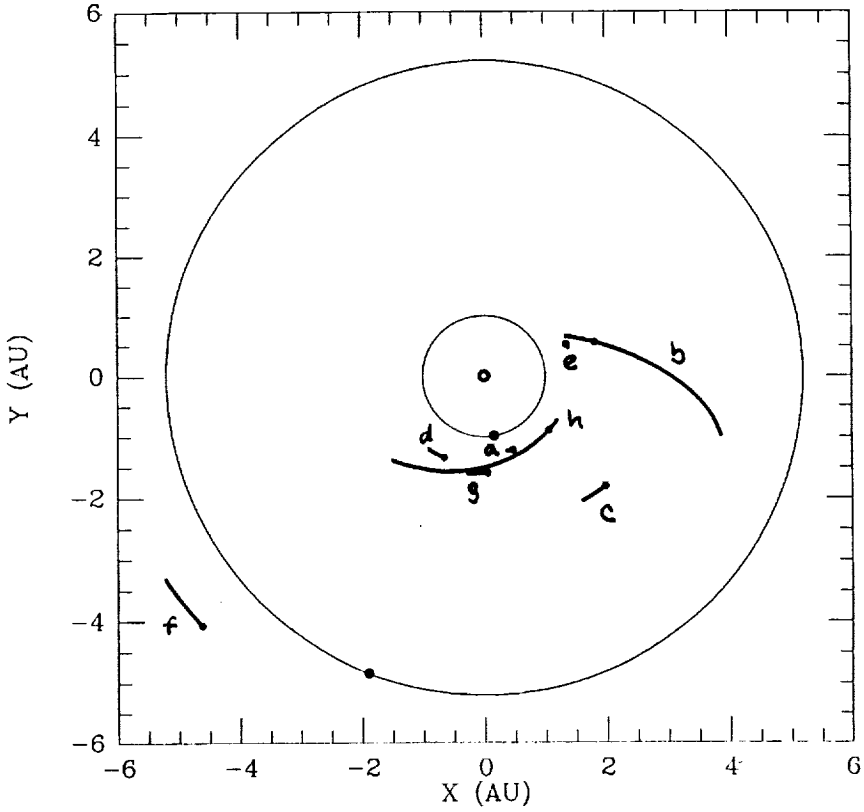

Figure 3. The location of the dust trails projected onto the ecliptic plane on July 1, 1983. The orbits and positions of the Earth and Jupiter are also shown. (a) Churyumov-Gerasimenko, (b) Encke, (c) Gunn, (d) Kopff, (e) Pons-Winnecke, (f) Schwassman-Wachmann 1, (g) Tempel 1, (h) Tempel 2.

orbits at epoch intervals corresponding to the times of the first and last scans used to construct the IRAS image. While the old software would constrain potential sources, the new software makes source identification essentially certain. In each case where a trail was identified, the new software yielded a projected orbit which was seen to have the same breaks and shifts in position as the associated trail (due to variations in the IRAS viewing geometry). The potential trail sources considered in this survey are given in Table 1.

Care had to be taken in the identification of some extended structures as trails. In (1), two trails, one of which had been tentatively identified as belonging to Shoemaker 2, the other belonging to an unidentified source, turned out to be diffraction spikes due to Jupiter (the planet was avoided in the scanning procedure, leaving a squarish void on the images from which the "trails" appeared to emerge). Similarly, diffraction spikes from Saturn were seen on an adjacent Map. Cirrus structures could also mimic the narrow appearance of trails over short distances, but were identified by their location remaining fixed between HCONs, while orbital motions of both the comet and the Earth would result in a parallactic shift between HCONs. Many faint candidate trails, seen in only one HCON, were rejected because of their correlation with the edges of cirrus structures seen at 100 μm.

TABLE 1. POTENTIAL PARENTS

Short-Period Comets

Arend
Arend-Rigaux
Ashbrook-Jackson
Biela
Boethin
Borrelly
Bowell
Bowell-Skiff
Bradfield
Brooks 2
Brorsen
Brorsen-Metcalf
Bus
Churyumov-Gerasimenko
Clark
Comas-Solá
Crommelin
D'Arrest
Daniel
De Vico-Swift
Denning-Fujikawa
Du Toit 1
Du Toit-Hartley
Du Toit-Neujmin-Delporte
Dubiago
Encke
Faye
Finlay
Forbes
Gale
Gehrels 1
Gehrels 2
Gehrels 3
Giacobini-Zinner
Giclas
Grigg-Skjellerup
Gunn
Halley
Haneda-Campos
Harrington
Harrington-Abel
Hartley-IRAS
Herschel-Rigollet
Holmes
Honda-Mrkos-Pajdušáková
Howell
IRAS
Jackson-Neujmin
Johnson
Kearnes-Kwee
Klemola
Kohoutek
Kojima
Kopff
Kowal 2
Kowal-Mrkos
Kowal-Vávrová
Longmore
Neujmin 1
Neujmin 2
Neujmin 3
Olbers
Oterma
Perrine-Mrkos
Peters-Hartley
Pons-Brooks
Pons-Winnecke
Reinmuth 1
Reinmuth 2
Russell 1
Russell 2
Russell 3
Russell 4
Sanguin
Schaumasse
Schuster
Schwassmann-Wachmann 1
Schwassmann-Wachmann 2
Schwassmann-Wachmann 3
Shajn-Schaldach
Shoemaker 1
Shoemaker 2
Slaughter-Burnham
Smirnova-Chernykh
Stephan-Oterma
Swift-Gehrels
Takamizawa
Taylor
Tempel 1
Tempel 2
Tempel-Swift
Tempel-Tuttle
Tritton
Tsuchinshan 1
Tsuchinshan 2
Tuttle
Tuttle-Giacobini-Kresák
Van Biesbroek
Väisälä
West-Kohoutek-Ikemu
Westphal
Whipple
Wild 1
Wild 2
Wild 3
Wirtanen
Wolf
Wolf-Harrington

Long-Period Comets

Austin (1982 VI)
Austin (1984 XIII)
Bowell (1982 I)
Bus (1981 XI)
Černis (1983 XII)
Elias (1981 XV)
Gonzales (1981 VII)
Hartley (1985 XIV)
Hartley-Good (1985 XVII)
IRAS (1983 I)
IRAS (1983 VI)
IRAS (1983 XVI)
IRAS-Araki-Alcock (1983 VII)
Levy-Rudenko (1984 XXIII)
Machholz (1985 VIII)
Meier (1984 XX)
Panther (1981 II)
Russell (1981 V)
Shoemaker (1983 XV)
Shoemaker (1984 XV)
Shoemaker (1985 II)
Shoemaker (1985 XII)
SOLWIND 2 (1981 I)
SOLWIND 3 (1981 XIII)
SOLWIND 4 (1981 XXI)
SOLWIND 5 (1984 XII)
Sugano-Saigusa-Fujikawa(1983 V)
Theile (1985 XIX)

TABLE 2.

TYPE I DUST TRAILS IN THE IRAS SKYFLUX PLATES

PLT/HCON		λ_0 (1950)	β_0 (1950)	λ_1 (1950)	β_1 (1950)	ΔMA_0	ΔMA_1	Comments*
56	1	124.387550	7.906315	128.463364	7.863007	1.13	-0.07	C-G (coma)
	1	133.924973	6.943444	135.137955	6.914125	0.36	-0.05	C-G (coma)
72	1	14.213708	5.153361	24.421719	6.503429	10.77	-11.63	Encke
	1	9.164062	3.925794	13.431341	4.546709	22.76	8.46	Encke
	2	9.671945	4.244484	24.170834	6.177160	23.83	-13.11	Encke
95	1	357.034424	1.865459	9.888929	4.029937	80.22	20.16	Encke
	2	359.726532	2.551209	9.889992	4.278696	66.68	22.99	Encke
	1	350.418793	-1.667467	6.074000	-6.074819	4.98	2.49	Tempel 2
	2	350.607300	-1.393038	358.859222	-3.713891	3.72	2.47	Tempel 2
	2	359.891174	-5.926529	5.574126	-7.469752	5.23	4.42	Tempel 2
96	1	5.121358	-5.844675	13.481600	-7.724786	2.69	1.06	Tempel 2
	1	14.048326	-10.946827	19.979362	-11.984856	4.04	2.95	Tempel 2
	2	4.380317	-7.134231	20.587673	-10.591124	4.58	1.65	Tempel 2
97	1	18.827351	-11.773843	35.877399	-13.423677	3.16	-1.01	Tempel 2 (coma)
	2	19.648220	-10.396776	28.721813	-11.630341	1.83	-0.34	Tempel 2 (coma)
	2	28.751648	-15.652569	35.026012	-15.827680	2.49	0.95	Tempel 2
98	1	34.650265	-13.432627	39.467449	-13.559826	-0.61	-2.16	Tempel 2
	1	41.794926	-14.133006	43.739124	-14.117133	-2.34	-3.04	Tempel 2
	1	43.691772	-17.164413	51.287430	-16.448332	-0.78	-3.58	Tempel 2
	2	33.841038	-15.779714	51.530251	-15.011994	1.24	-4.86	Tempel 2 (coma)
	3	34.479713	-21.480413	50.227848	-19.799938	3.25	-1.83	Tempel 2 (coma)
99	1	50.047771	-16.546680	55.164597	-15.908616	-3.10	-5.37	Tempel 2
107	1	176.058655	6.956966	186.532608	5.016053	5.53	2.92	Tempel 1
	2	178.954361	5.990831	186.828445	4.496393	6.19	4.17	Tempel 1
	2	178.985260	4.924236	186.557709	5.205716	17.42	13.55	Kopff
108	1	195.193710	12.554204	199.976624	12.513857	36.81	33.77	Tempel 2
	1	185.370697	5.270563	193.422974	3.472945	3.16	1.47	Tempel 1
	1	195.878586	2.264314	202.303894	0.768320	4.26	2.87	Tempel 1
	1	187.513855	5.626348	193.831863	5.774901	11.99	9.66	Kopff
	1	195.865234	4.814285	202.985992	4.797383	11.61	9.07	Kopff
	2	191.543045	13.666253	199.244110	13.924667	37.03	32.06	Tempel 2
	2	185.380035	5.166706	202.743652	5.408048	14.08	7.50	Kopff
	2	185.636765	4.739122	202.496796	0.813562	4.42	0.88	Tempel 1
109	1	198.540802	12.546599	216.582169	11.394038	34.63	25.85	Tempel 2
	1	201.798843	4.822292	212.507645	4.578817	9.43	6.31	Kopff
	2	198.041077	13.904992	208.393890	13.822097	32.73	27.48	Tempel 2
	2	208.832260	11.243883	217.019012	10.324701	30.70	27.17	Tempel 2
	2	201.566559	5.402317	208.193054	5.338406	7.89	6.00	Kopff
	2	208.976532	4.295098	211.366806	4.231767	8.55	7.86	Kopff
	3	212.632690	9.037502	217.713852	8.379668	36.17	33.85	Tempel 2
110	1	215.396149	11.520839	223.549469	10.357949	26.34	23.53	Tempel 2
	2	215.786194	10.503631	225.365738	8.870387	27.59	24.29	Tempel 2

	3	216.492935	8.558039	221.799957	7.775908	34.37	32.17	Tempel 2
116	1	314.062927	9.411806	322.978821	6.810231	7.37	6.19	Tempel 2
117	1	322.497925	6.959069	337.249176	2.523213	6.27	4.23	Tempel 2
	2	323.204590	6.088303	328.661072	4.500309	4.91	4.51	Tempel 2
	2	328.974579	5.258886	337.291046	2.716496	5.26	5.97	Tempel 2
118	1	336.545135	2.726181	351.577728	-2.059085	4.29	4.85	Tempel 2
	2	336.358246	3.050694	351.793274	-1.723108	6.11	3.57	Tempel 2
120	1	0.226384	-22.056042	7.463731	-22.978146	2.15	0.	P-W (coma)
	2	3.768632	-26.808037	12.681046	-26.610825	2.58	-0.18	P-W (coma)
131	1	188.984299	-8.754807	193.008530	-9.088462	8.29	4.07	S-W 1
	2	188.211716	-8.521176	192.995987	-8.911768	9.56	4.52	S-W 1
132	1	191.096420	-8.938723	193.495087	-9.127597	6.05	3.56	S-W 1
	1	195.083572	-8.776935	198.177383	-8.956430	3.17	0.	S-W 1 (coma)
	1	200.640717	1.184829	204.907516	0.134709	3.20	2.32	Tempel 1
	2	191.096893	-8.761195	197.404358	-9.201373	6.52	0.	S-W 1 (coma)
	2	200.589355	1.304591	205.083603	0.137821	1.22	0.46	Tempel 1
133	1	203.282059	0.548697	222.473938	-4.339222	2.64	-0.84	Tempel 1 (coma)
	1	209.414841	4.644820	219.148911	4.332558	7.15	4.70	Kopff
	2	203.188553	0.618127	208.188950	-0.688356	0.79	-0.08	Tempel 1 (coma)
	2	209.014923	-0.632426	222.271683	-3.889977	2.98	0.46	Tempel 1
	2	208.974792	4.308023	219.424606	3.873339	8.55	5.86	Kopff
	3	212.973709	3.430291	219.626923	3.142338	12.87	11.03	Kopff
134	1	224.109314	8.067718	234.164856	5.824548	27.05	23.87	Tempel 2
	1	220.107758	-3.710375	223.197968	-4.538164	-0.44	-0.98	Tempel 1
	1	224.208176	-3.526715	231.101059	-5.078986	2.31	0.96	Tempel 1
	1	217.508804	4.379894	223.451324	4.076388	5.11	3.79	Kopff
	1	224.222595	3.230187	234.912003	2.502056	6.61	4.29	Kopff
	2	223.210526	9.307357	233.926758	6.887533	24.96	21.95	Tempel 2
	2	219.914001	-3.286891	229.645157	-5.645858	0.89	-0.78	Tempel 1 (coma)
	2	217.764145	3.978576	234.866165	2.900977	6.18	2.63	Kopff
	3	219.654144	8.090461	234.053085	5.381752	33.05	28.37	Tempel 2
	3	217.988266	3.223224	234.124741	2.273944	11.46	7.86	Kopff
135	1	233.236801	2.604616	238.481979	2.209785	4.60	3.56	Kopff
	2	233.210327	3.037457	235.367691	2.851344	2.92	2.53	Kopff
	3	233.434265	2.309254	238.875137	1.951485	8.06	7.62	Kopff
138	1	284.144073	13.877756	293.333008	12.070649	9.33	7.66	Tempel 2
	2	282.416809	13.081878	293.234039	11.025568	8.52	6.41	Tempel 2
139	1	291.904602	12.360771	308.004883	8.773201	7.90	5.20	Tempel 2
	2	291.763245	11.287588	298.723297	9.845864	6.65	5.34	Tempel 2
	2	298.783600	11.957493	301.677429	11.269445	7.94	7.47	Tempel 2
	2	303.298218	11.431726	308.372803	10.130794	7.82	7.06	Tempel 2
140	1	306.546906	9.108483	313.228210	7.438509	5.41	4.30	Tempel 2
	1	314.056885	9.393433	322.723969	6.870560	7.37	6.23	Tempel 2
	2	308.835175	9.978965	322.256378	6.335083	6.98	5.02	Tempel 2
141	1	322.275513	7.017034	332.278351	3.982780	6.30	4.90	Tempel 2
	1	326.495453	-9.739374	332.947083	-10.155661	5.88	2.54	Gunn
	2	321.541931	6.550813	328.217712	4.641628	5.15	4.14	Tempel 2
142	1	330.790802	-10.026687	337.992981	-10.360558	3.69	-0.26	Gunn (coma)
	2	330.288818	-10.337832	331.027100	-10.385697	4.49	4.10	Gunn
	2	333.522858	-10.996874	337.828979	-11.158563	3.47	1.19	Gunn
158	1	228.957077	-4.605928	237.971909	-6.614661	1.37	-0.33	Tempel 1 (coma)
162	3	275.634857	-1.133098	291.783691	-2.371355	1.41	-0.45	Kopff (coma)

Trails Having Unknown Parents (Orphans)

4	3	55.214	98.258	53.442	91.351	(coma?)
54	1	4.163	98.219	4.565	102.900	
107	1	7.231	177.677	6.246	181.563	
110	3	12.287	218.284	12.342	219.798	
119	1	-10.323	4.166	-9.940	359.738	
123	1	-39.830	57.975	-40.745	56.462	
135	1	1.540	240.756	6.912	235.213	(coma?)
171	3	-59.523	48.185	-66.223	39.515	
188	2	-64.234	338.784	-65.355	356.874	

**Notes*

C-G = Churyumov-Gerasimenko
P-W = Pons-Winnecke
S-W 1 = Schwassmann-Wachmann 1
(coma) = The cometary coma is seen within the trail segment.

The results of the trail survey are shown in Table 2, and are being incorporated into a major paper on trails (Sykes and Walker, in perparation). Short-period comets are the only solar system objects which were found to have trails. In all, eight trails were detected in association with known short-period comets (Table 2), and several faint trails were detected which did not appear to be associated with the orbit of any known object (a comparison with the projected orbits of all known main-belt asteroids, however, has not been made). The location of all detected trails projected onto the plane of the ecliptic on July 1, 1983 is shown in Fig. 2. The most extended trails are Encke, Schwassmann-Wachmann 1, and Tempel 2. Whenever the coma of a short-period comet was observed on a Skyflux Plate, a trail was also detected. On the other hand, no long-period comet had a detectable trail. Comet Bowell (1982 I) was seen to have a large *tail*, but otherwise, the long-period comets appeared as fuzzy point sources.

Tempel 2

An exhaustive examination was begun of the Tempel 2 dust trail (6) and continues. Tempel 2 was the most extensively observed trail during the IRAS mission, as well as the brightest. This was due to the fact that during the IRAS mission, Tempel 2 passed through both perihelion and perigee at about the same time. A comparison of the trail position with calculated syndynes indicates that the trail is composed of particles larger than 1 mm. Dynamical calculations suggest that the trail particles have a velocity less than several meters per second relative to the parent comet, and that forward of the comet's orbital position, trail particles have diameters $\sim$ 6 mm (assuming unit mass density). Initially, trail particles were found to be extremely dark (7), but more accurate measurements of trail fluxes from the analysis of individual detector scans yielded the remarkable result that the trail particles exhibit a small, but significant, excess in color temperature relative to that expected for a blackbody at the same heliocentric distance. They must either support a temperature gradient across their sunlit surfaces, or act as parents or carriers of particles $< 100\mathring{A}$ in diameter (which cannot have come from the comet nucleus directly because of acceleration to km/sec velocities while they are coupled to the gas outflow). In either case, this suggests that trail particles are fluffy or low density, which in turn suggests that the surfaces of comet nuclei are also fluffy or low-density.

Zodiacal Dust Bands

A major work on the relation between the zodiacal dust bands and main belt asteroid families was also completed under this contract (12). This involved the development of a mathematical model of the volume density of a dust band torus, given an ensemble of particles possessing identical orbital elements (a, e, i). The effects of dispersion in orbital elements on the morphology of the dust band tori were determined and used to generate a scan-by-scan mapping of the half-power points associated with the volume density peaks (which we see as pairs of bands) onto the IRAS data. This allowed for an accurate comparison of the dust band structures seen in the data with bands expected to be found a

priori in association with 8 major asteroid families identified by Williams (13).

The two brightest bands (β and γ) were associated with the Koronis and Eos asteroid families, respectively, while the relatively faint and most central band (α) was shown to be associated with the Themis family. Four other faint band pairs, previously discovered (11), were found not to be associated with any major family with the possible exception of the Io family.

It was determined (12) that dispersion in the orbital elements of the dust band tori particles resulted in a decreased separation of the locations of peak particle number density. When viewed from the Earth, this translates to a pair of bands being seen at lower latitudes. This effect was measured for the dust associated with the Eos family, which was found to have twice the dispersion of the asteroid members of the family. Understanding this effect, which arises from collisional diffusion, was critical to the identification of the γ bands with the Eos family.

Another interesting result was the determination that the Eos and Themis families are significantly older than the Koronis family. That is, by applying models of the collisional evolution of the surface area of dust bands, and applying these models to the IRAS observations, it was determined (12) that the catastrophic disruption of the Koronis family parent body occured much later than the disruption of the Eos and Themis parent bodies. This is supported by independent studies of the distribution of rotation rates among these asteroids (14).

It appears that dust in the asteroid belt is being primarily generated within the Eos and Koronis asteroid families (12). Since asteroid collisions may be a principal source of the zodiacal cloud, some thought was given to the implications of relatively well-localized sites of dust production in the asteroid belt. This resulted in speculation (16) that a dust collection experiment at Earth would experience modulations in the interplanetary dust flux as the dust from the asteroid belt evolves past the Earth, and that it may be possible to isolate the components of the interplanetary dust complex coming from these specific source regions. Hence it may be possible to identify samples corresponding to definite asteroid taxonomic types, primarily S (Koronis) and K (Eos). This is very important since S type asteroids are one of the most prominant and populous taxonomic groups, and has no generally agreed upon meteoritic analog.

Other

Some work was undertaken as a target of opportunity when local access to the IRAS Pointed Observations became available to the PI. In this mode, IRAS made a number of serendipitous observations of asteroids and comets (15). We determined that while in this mode, IRAS scanned the locations of over 200 known asteroids and 15 comets. It also scanned an undetermined number of undiscovered asteroids and comets. Of the asteroids detected in the Pointed Observations, 56 were also observed in survey-mode and had been included in the IRAS Asteroid and Comet Survey. 49 additional asteroids were also detected, and represent a new contribution to the total number of asteroids having radiometric observations. The identification of previously undiscovered solar system

objects has been proposed in a separate grant proposal as the critical part of an effort to identify variable astrophysical sources in the Pointed Observations.

References

(1) Sykes, M., *et al.* 1986. *Science* **232**, 1115.
(2) Low, F., *et al.* 1984. *Astrophys. J.* **278**, L19.
(3) Davies, J., *et al.* 1984. *Nature* **309**, 315.
(4) Eaton, N., *et al.* 1984. *MNRAS* **211**, 15P.
(5) Sykes, M., *et al.* 1986. *Adv. Sp. Res.* **6**, 67.
(6) Sykes, M., *et al.* 1990. *Icarus* **86**, 236.
(7) Sykes, M. 1988. In *Comets to Cosmology*, p. 66.
(8) Dermott, S., *et al.* 1984. *Nature* **312**, 505.
(9) Sykes, M. and R. Greenberg. 1986. *Icarus* **65**, 51.
(10) Sykes, M., *et al.* 1989. In *Asteroids II*, p. 336.
(11) Sykes, M. 1988. *Astrophys. J.* **334**, L55.
(12) Sykes, M. 1990. *Icarus* **84**, 267.
(13) Williams, J. 1979. In *Asteroids*, p.1040.
(14) Binzel, R. 1986. *Collisional evolution in the asteroid belt: an observational and numerical study.* Thesis, University of Texas, Austin.
(15) Sykes, M. and R. Cutri. 1989. *B.A.A.S.* **21**, 963.
(16) Sykes, M. 1989. *Meteoritics* **24**, 330.

PUBLICATIONS UNDER CONTRACT

Papers

1. Sykes, M. (1990). Zodiacal dust bands: their relation to asteroid families. *Icarus* **84**, 267.
2. Sykes, M., R. Walker, and D. Lien (1990). The Tempel 2 dust trail. *Icarus* **86**, 236.
3. Sykes, M. and R. Walker (1991). Cometary dust trails. I. Survey. In preparation.

Invited Reviews

4. Sykes, M., R. Greenberg, S. Dermott, P. Nicholson, J. Burns, and T.N. Gautier (1989). Dust bands in the asteroid belt. In *Asteroids II* (R. Binzel, T. Gehrels, M. Matthews, eds.), University of Arizona Press, Tucson, p. 336.

Abstracts

1. Sykes, M.V. and R.M. Cutri (1989). The IRAS Deep-Sky Survey of Asteroids. *Bull. Am. Astr. Soc.* **21**, 963.
2. Walker, R.G., M.V. Sykes, and D.J. Lien (1989). Thermal properties of dust trail particles. *Bull. Am. Astr. Soc.* **21**, 967.
3. Sykes, M.V. (1989). Asteroidal sources of dust at the earth's orbit. *Meteoritics* **24**, 330.

Invited Talks

"IRAS: Accomplishments and Discoveries in Planetary Science." Presented at the XXVIII COSPAR, The Hague, Netherlands. June 26, 1990.

"IRAS: Accomplishments and Discoveries in the Solar System." Seminar given at the Royal Observatory, Edinburgh, Scotland. June 28, 1990.